https://dx.doi.org/10.4314/ijs.v23i1.13

ADSORPTION OF METHYLENE BLUE ON CORNCOB CHARCOAL: THERMODYNAMIC STUDIES

Fodeke, A. A.* **and Ayejuyone, O. J.**
Department of Chemistry, Obafemi Awolowo University, Ile-Ife, Osun State
* Corresponding author. E-mail: afodeke@yahoo.co.uk; aafodeke@oauife.edu.ng; Tel: +234 7083519273
(Received: March 3, 2021; Accepted March 29, 2021)

ABSTRACT

To obtain the thermodynamic properties of adsorption of methylene blue (MB) on corncob carbonaceous adsorbents - untreated (UCC) and acid treated (TCC) - their equilibrium adsorption was determined between 10 – 40 °C at different pH conditions. The adsorption isotherms were fitted to Freundlich, Langmuir and Temkin isotherm models. The point of zero charge of each of the adsorbents was also determined. The point of zero charge was 10.58 ±0.09 for TCC, and 7.55 ± 0.10 for UCC. Only Freundlich model could account for the observed thermodynamic properties of MB adsorption by the adsorbents, though Temkin and Langmuir models have higher correlation coefficients. MB adsorption by TCC was an entropically driven process which depends on pH; ΔS^{o} at pH 10.5 < ΔS^{o} at pH 8.0 <ΔS^{o} at pH 12.0. The ΔH^{o} of the endothermic process at pH 12 is > ΔH^{o} at pH 8 > ΔH^{o} at pH 10.5. The results suggest that MB adsorption by the adsorbents occur by physisorption and is optimum when the pH is around the point of zero charge. It is important to ensure that in addition to fitting and equilibrium adsoption data by an isotherm model, the fit of the relevant equilibrium parameter should also be good and give thermodynamic quantities that could satisfactorily account for the observed adsorption properties of the system. Deciding the suitability of an isotherm model for fitting adsorption equilibrium experiment based on compared error function of the fitted curves or lines through single temperature isotherm could lead to erroneous conclusion.

Keywords: adsorption, adsorbent; methylene blue; enthalpy; entropy; Freundlich

INTRODUCTION

Dyes have found great use in several human activities such as textile, paper, paint, cosmetics, additives in food and many other uses. A large amount of these dyes find their way into water bodies where they cause harm for aquatic life and make the water unfit for human consumption. In the search of a cheap and sustainable means of removing dye pollutants, several researchers have embarked on experiments aimed at finding methods, optimum conditions and materials that can be used for efficient dye removal (Malik *et al*., 2007; Suteu *et al*., 2011; Garg *et al*., 2004; Adegoke *et al*., 2015; Amodu *et al*., 2015).

Removal of dyes and metallic ions from wastewater has stimulated significant interest in the use of synthetic polymers. Materials such as polyphynylamine (Amodu *et al*., 2015), poly(cyclotriphosphazene-co-4,4 - sulfonyldiphenol) nano tubes (Ayad *et al.,* 2012; Chen *et al*., 2014) and carbon based materials from agricultural wastes (banana peel, cassava peel, rice bran, periwinkle shell, corncob and palm kernel husk) have been employed in water purification (Kumur *et al*., 2008; Bello *et al*., 2008; Rajeshwarisivaraj *et a*l., 2001). While much of the work in the past had been dedicated to finding the most suitable kinetic and adsorption model for fitting data from adsorption experiments (with the hope of ascertaining the mechanism of adsorption), the suitability of the equilibrium adsorption model had often been predicated on the goodness of the fit of a given adsorption isotherm model used in fitting the experimental data. Little data is available on the systematic studies of the relationship between fitting model and the thermodynamics of adsorption of adsorbates on adsorbents. Where such studies were carried out, adsorption properties of the adsorbates and adsorbents are often not related quantitatively or semi-quantitatively to the thermodynamic quantities obtained.

To remove ambiguity that may arise from the shortcomings described above, we undertake to: (i) determine how adsorption of MB on corncob charcoal are affected by pH at the point of zero charge of the adsorbent and also above and below it; (ii) estimate the effect which acid treatment of corncob charcoal had on its adsorption properties compared to the untreated corncob; (iii)

determine which adsorption isotherm best fit the equilibrium data of the adsorption of MB on each of the two adsorbents used; (iv) account for the observed adsorption properties using the thermodynamic information obtained from the equilibrium data.

The point of zero charge of acid treated and untreated carbonized corncobs charcoals were determined and the equilibrium adsorption studies of MG on the two adsorbents were carried out at a pH below, around and above the point of zero charge of the adsorbents. The equilibrium adsorption data were then fitted to linear form of three adsorption models including; Freundlich, Langmuir and Temkin. The standard enthalpy and entropy change accompanying the adsorption were obtained from the van't Hoff plot of the temperature dependent model constants from each model. The most suitable model was rationalized using a combination of minimum error function of the van't Hoff plot and the correlation between the observed adsorption behavior of the system and the thermodynamic parameters from van't Hoff plots of the adsorption constant from each of the isotherm model against the temperature of the experiment.

Adsorption Isotherms and Data Analyses

The experimental data were subjected to each of the adsorption isotherms which are briefly discussed as follows.

Freundlich model: Linearized form of Freundlich isotherm has been mathematically expressed as (Freundlich, 1906),

$$\ln q_e = \ln K_F + \frac{1}{n}\ln(C_e) \qquad (1)$$

Where q_e is the mass of MB per unit mass of adsorbent (mg g^{-1}) at equilibrium, C_e is the equilibrium concentration of MB, n and K_F are the Freunlich constants related to the adsorption intensity and adsorption capacities. Adsorption in which adsorbents have high affinity for the adsorbates are characterized by high value of n (Kano *et al*, 2000).

Langmuir model: Linear form of which is expressed as (Langmuir, 1916),

$$\frac{1}{q_e} = \frac{1}{K_L q_m}\frac{1}{C_e} + \frac{1}{q_m} \qquad (2)$$

Here, K_L and q_m are the Langmuir constant and the maximum adsorbate per unit mass of adsorbent (mg g^{-1}) respectively.

Temkin model: the linearized form of which is expressed as (Temkin and Khim, 1914),

$$q_e = \frac{RT}{B_T}\ln K_T + \frac{RT}{B_T}\ln C_e \qquad (3)$$

In Temkin model, R and T are gas constant (8.314 J K^{-1} mol^{-1}) and absolute temperature respectively. The Temkin constants B_T is related to the adsorption heat whereas K_T is related to the maximum energy of binding.

The equilibrium adsorption constants of each of the model isotherm can be related the thermodynamic expression according to:

$$\ln K_X = -\frac{\Delta H}{RT} + \frac{\Delta S}{R} \qquad (4)$$

where the subscript X = F (for Freundlich), T (for Temkin) or L (for Langumuir) constant.

In the limit of constant value of ΔH within the temperature range of the experiment, the enthalpy change ΔH and ΔS the entropy change can be obtained from the plot of $\ln K_X$ against reciprocal of the temperature measured in Kelvin. Under standard conditions, it would therefore be possible to determine the standard free energy change at different temperature from the thermodynamic expression:

$$\Delta G^\circ = \Delta H^\circ - T\Delta S^\circ \qquad (5)$$

where ΔG° is the change in standard free energy at temperature T. ΔH° and ΔS° are the respective change in standard enthalpy and entropy.

MATERIALS AND METHODS

Materials

The UV-1800 spectrophotometer, Shimadzu, Europa GmbH, was used for absorbance measurement. Grant circulating thermostated water bath was used to keep the spectrophotometer at the desired temperature. CC-60 Cryocool, a product of Thermoscientific Neslab was used to maintain a desired

temperature. Model Ov-160 Gallenkamp oven used was made in England. The Benchtop pH meter HI 2209 was made by Hanna Instrument Inc., USA. Samples were weighed using New Classic ML54 Mettler Toledo Analytical balance. Methylene blue (MW = 319.85 g mol^{-1}) a product of Sigma Aldrich, India was used without further purification.

Determination of Point of Zero Charge

Point of zero charge (PZC) of pulverized corncob charcoal (≤ 250 x 10^{-6} m) was determined using the salt addition method (Tan *et al.*, 2008; Bakatula *et al.*, 2018). The pH of solutions of 0.1 mole dm^{-3} sodium chloride in 50 cm^3 flask were adjusted to 2.0 ≤ pH ≤ 12 using either 0.1 mol dm^{-3} hydrochloric acid or sodium hydroxide. 20 cm^3 of the solution of specific pH was measured into two caped vials. At known pH, 0.1 g of UCC, detailed preparation of which had been described earlier (Fodeke and Olayera, 2019) was weighed into one of the vials (no charcoal was added to the other meant to serve as control at a specified pH). The content of the two vials were shaken, then, allowed to settle for 12 hours. The pH of the solution in each vial was then determined. The pH of the solution without carbonaceous adsorbent was designated pHi while the pH of solution containing the adsorbent was designated pH_f. The experiment was carried out in triplicate. The mean value of change in pH designated ΔpH was calculated by subtracting the pH in the presence of adsorbent after equilibration, pH_f, from pH_i, the solution pH in the absence of adsorbent. ΔpH was plotted against pH_i to estimate the PZC.

Molar Extinction of Methylene Blue

The molar extinction coefficient of MB was determined in the range 3 ≤ pH ≤ 9 by measuring the absorbance of accurately prepared solution of MB (1 x 10^{-6} mol dm^{-3} – 10 x10^{-6} mol dm^{-3}) in each buffer solution. The absorbance of each solution was plotted against the concentration of the MB. Each investigation was repeated twice and the mean of the absorbance was plotted against concentration. The molar extinction coefficient was obtained from the slope of the plot.

Equilibrium Adsorption Measurement

Carbonized corncob charcoals were obtained as described previously (Fodeke and Olayera, 2019). Equilibrium adsorption was also determined using the method described earlier (Fodeke and Olayera, 2019). Increasing mass of adsorbent (0 – 0.02 g) was added to 20 cm^3 of 47.5 x 10^{-6} mol dm^3 of methylene blue dye (MW = 696.665 g/mol). The mixtures were shaken and then allowed to equilibrate at a given temperature in buffer of specified pH for 12 hours. The experiment was carried in the temperature range 10 – 40 °C in triplicate. For UCC, the solution pH were 5, 7.2 and 9.0. TCC experiment was carried out in solutions of pH 8.0, 10.5 and 12. Absorbance (Abs^{666}) was measured at 666 nm and the concentration of dye left at equilibrium at a given pH was obtained using the experimentally determined value of extinction coefficient (ε^{666}) at the corresponding pH. The percentage dye removed was then calculated using Eq. (6) and qe is obtained from Eq. (7) which are respectively given as follows;

$$\% \text{ MB adsorbed} = \frac{\text{Initial concetration of MB} - \text{Concentration of MB at equilibrium}}{\text{Initial concetration of MB}} \times 100\% \quad (6)$$

$$q_e = \frac{\text{Initial dye conc.}(mg/dm^3) - \text{dye conc. at equilibrium } (mg/dm^3)}{\text{mass adsorbent in g}/dm^3 \text{ of solution}} \quad (7)$$

RESULTS AND DISCUSSION

Point of Zero Charge

The plots for the determination point of zero charge of UCC and TCC are presented in Fig. 1 (a and b). It can be seen that ΔpH decreases with increasing pH in each case. A minimum occurred in the case UCC at pH ca. 10, before increasing (Fig. 1a), whereas, no such minimum is observed in TCC (Fig. 1b). The pH at which ΔpH is zero is the point of zero charge. For UCC this value is 7.55 but for TCC it is 10.58.

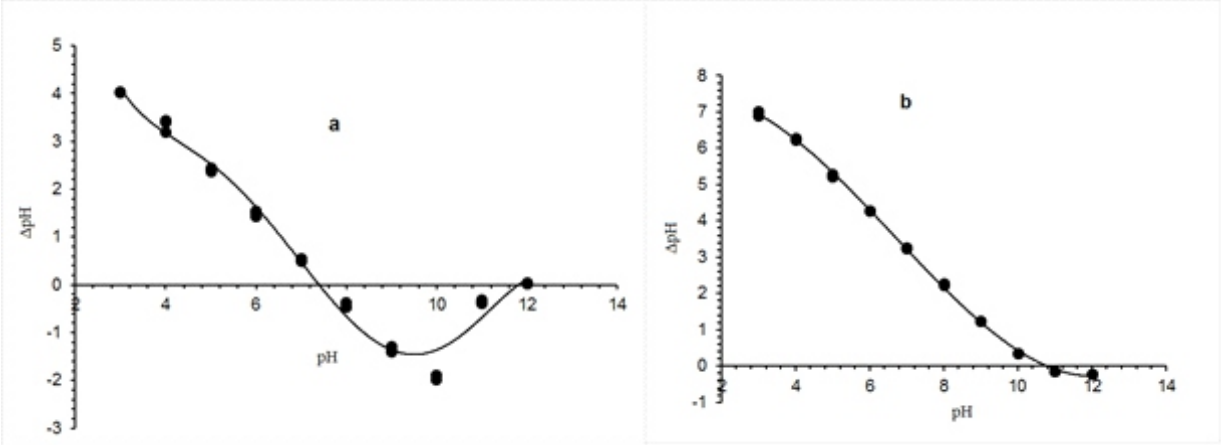

Figure 1: The dependence of change in pH caused by addition of 0.1 g of (a) UCC (b) TCC, against initial pH of solution. Volume of the solution was 20 cm^3 and the ionic strength was 0.1 mole dm^{-3} NaCl. Each experimental data point is the mean of three replicate experiments.

Effect of pH on the Molar Extinction Coefficient of MB

The dependence of molar extinction of MB on pH is presented in Fig. 2. It can be seen that absorbance of MB is pH dependent at 666 nm. The molar extinction coefficient increases gently from the value at pH 3 to the highest at pH *ca.* 5 and reduces slightly at lower pH, but decreases more significantly with increasing pH. This dependence of molar extinction coefficient of MB may be due to variation in degree of aggregation of MB under different pH conditions. It had previously been shown that MB form aggregates; including dimers and trimers, to different extent depending on pH and different concentrations (Golz and Vander Griend, 2013; Fernandez-Pe´rezand Marba´n, 2020). We therefore posit that the higher molar absorptivity under low pH conditions might suggest that MG exist as dimer or trimers which dissociates into the monomers with increasing pH. In other words, an equilibria involving the monomer, dimer and trimer must have been responsible for the variation in the molar absorptivity of MG. This findings suggests that it is important to determine or use the correct molar extinction coefficient at any particular pH of experiment because the pH has capability for altering the aggregation state of the dye. This may directly alter the adsorption of MG to surfaces and as well as affect the molar extinction coefficient which are used in the estimation of the concentration. Using incorrect molar extinction coefficient in calculating the dye concentration left at equilibrium in an adsorption experiment could result in introduction of additional errors which may result in wrong conclusions from the experiment. Having an idea of the state of aggregation of the MG under different pH conditions should therefore be important in providing explanation on the difference that may be observed in the adsorption of behavior of the dye under different pH conditions.

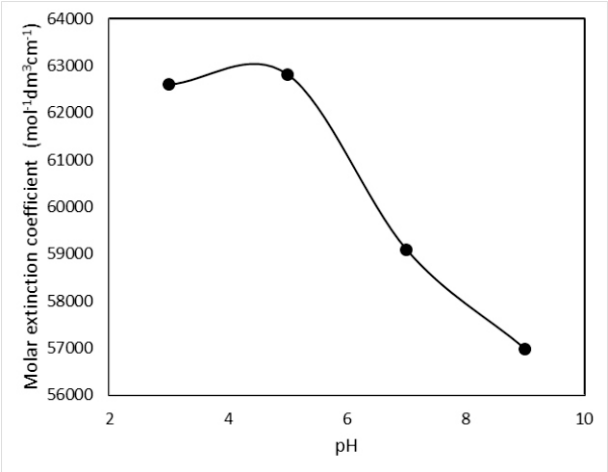

Figure 2: The dependence of molar extinction coefficient of MB on pH of buffer solution at 25 °C. Wavelength of measurement is 666 nm. Each experimental data point is the mean of three replicate experiments.

Effect of Temperature on Adsorption of MB by UCC

The percentage MB removed by UCC as a function of adsorbents dosage are presented in Fig. 3(a-c). For clarity, though the experiment was carried out at seven temperatures, only data obtained at temperatures 10, 20, 30 and 40 °C are presented. Fig 3a presents data collected at pH 5.0. Corresponding data in Figs. 3b and 3c were collected at pH 7.2 and 9.0 respectively. It can be seen that the percentage MB adsorbed do not show any specific pattern when the effect of temperature variation on the adsorption capacities are considered are compared at different pHs. However it is clear that pHs 5 and 9 the adsorption percentage adsorption is best at 40 °C. At pH 9.0 it is obvious that percentage dye adsorbed increases with increasing temperature.

Effect of pH on Adsorption of MB by UCC

At pH 5.0 the maximum percentage adsorption, at adsorbent dosage of 0.8 g dm^{-3} (the maximum adsorbent dosage) is about 57.3%. At pH 7.2 the maximum proportion of dye adsorbed was *ca.* 80.7% (at 10°C). At pH 9.0 (Fig. 3c) however, the maximum percentage of MB adsorbed was *ca.* 81.3 (at 40°C). These observations suggest that the efficiency of UCC as adsorbents increases with increasing pH, although the adsorption capacities at pH 7.2 and 9.0 are quite close. The higher percentage of adsorbate removed from the equilibrium solution at pHs 7.2 (Fig. 3b) and 9.0 (Fig. 3c) compared to solution at pH 5.0 (Fig. 3a) may be due to the interplay of the roles of both electrostatic interaction and hydrophobicity resulting from uncharged moiety of the dye in relation to the point of zero charge (7.55 for UCC). Though pH 7.2 is closer to the point of zero charge and the adsorption efficiency should be higher at this pH. Being is more acidic than pH 9.0, MB would be more positively charged rather than neutral compared to that at pH 9.0. The interplay of the roles of both the electrostatic contribution and the closeness of the pH conditions to the point of zero charge to the adsorption efficiency might be responsible to the similarity in the adsorption capacity of UCC for MB in spite of the difference in pH. However, at pH 5.0, the adsorption capacity of the dye for UCC is significantly less, because of the electrostatic repulsion which is expectedly between neighbouring positively charged MB on the adsorbent in a more acidic medium.

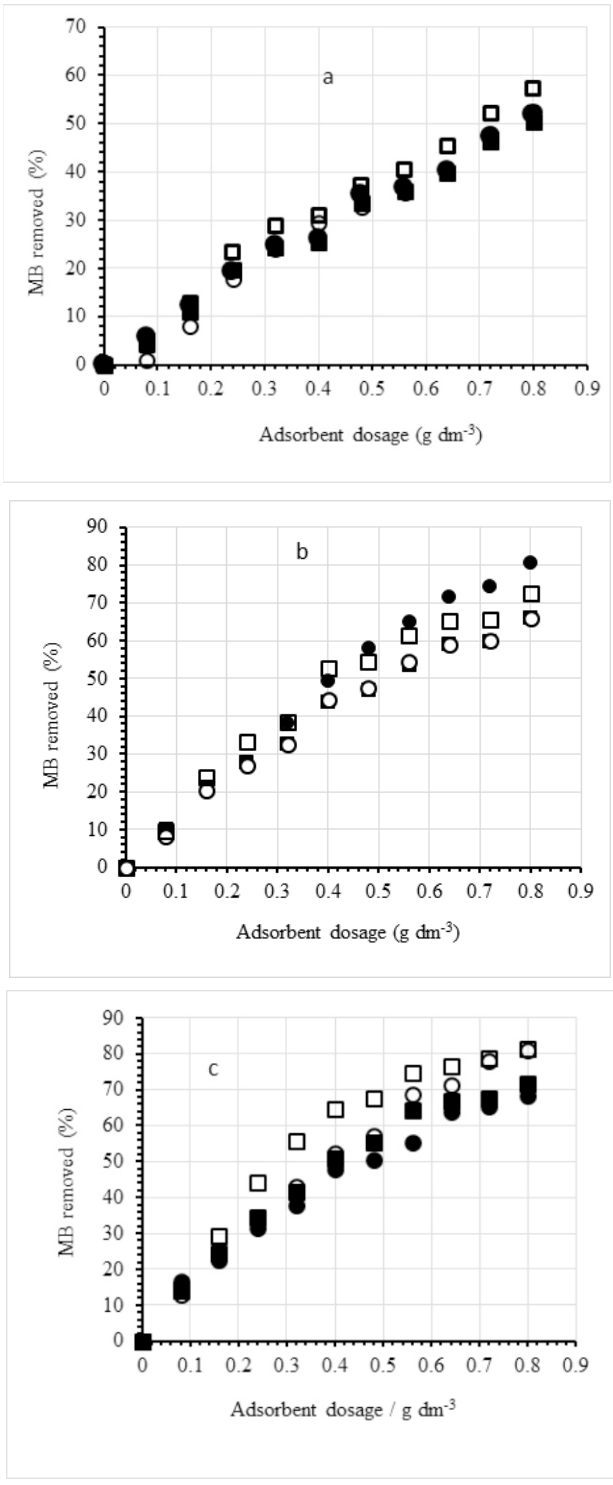

Figure 3: Percentage dye removed as a function of the UCC dosage at 10 °C, filled circle; 20 °C, filled square; 30 °C, open circle; 40 °C, open square. The pH conditions are panel (A) 5.0, (B) 7.2 and (C) 9.0. Initial dye concentration was 47.5 x 10^{-6} mol dm^{-3}, ionic strength was 0.1 mol. dm^{-3} (NaCl). Each experimental data point is the mean of at least three replicate experiments.

Effect of Temperature on Adsorption of MB by TCC

Experimental data point for the dependence of percentage dye adsorbed on TCC dosage is presented in Fig. 4 (a – c). Fig. 4a presents the adsorption of MB by TCC at pH 8. Corresponding data at pH 10.5 and pH 12 are presented in Figs. 4b and 4c respectively. It can be seen that adsorption of MB on TCC increases with the dosage of the adsorbent in each case but attains a maximum of 97 % or higher at adsorbent dosage ranging from 0.4 to 0.6, depending on the pH of the solution. Close examination of the Figures revealed two things; first is that percentage MB removed increases with increasing temperature until the maximum adsorption is achieved. The second is that at very low dosage, the difference between the adsorption capacities at different temperatures is higher. This difference diminishes with increasing dosage of adsorbent.

Effect of pH on Adsorption of MB by TCC

The highest percentage adsorbate removed under each conditions of pH is 99.01 at pH 10.5 (Fig. 4b), 98.4 at pH 8.0 (Fig. 4a) and 97.1 at pH 12 (Fig. 4c). These values of percentage adsorption were much higher than those observed in UCC. It is obvious in this case that the highest adsorption capacity occurred at pH closest to the point of zero charge of the adsorbent.

Effect of Acid Treatment on Corncob charcoal

Comparing the experimental data for the adsorption of UCC with TCC (Fig. 3 with Fig. 4) revealed that the percentage MB adsorbed by TCC were generally higher compared to UCC under identical conditions of temperature and adsorbent dosage (though the pH are different). Whereas, the maximum percentage adsorption of MB by UCC was about 81.3 (at pH 9.0) at the maximum adsorbent dosage (0.8 g dm^{-3}), for TCC, at pH 12 (the pH at which optimum adsorption of the adsorbent is least), the optimum adsorption value of *ca.* 97.1 % was reached at adsorbent dosage of *ca.* 0.6 gdm^{-3}. This gives an indication that the acid treatment given to corncob charcoal in producing TCC significantly increased its usefulness as an adsorbent. More than 99% of the dye adsorbate was removed at pH 10.5 (at dosage as low as 0.5 g/dm^3), meaning that small quantity of the adsorbent (*ca.* 0.5 g in 1 dm^3) will effectively remove the dye concentration as high as *ca.* 50×10^{-6} mol dm^{-3}. The findings that TCC at pH 8.0 has higher adsorption capacity than UCC at pH 9.0, suggests that the difference in the adsorption capacities of the two adsobent neither arises solely from the difference in the pH condition nor from the difference between the pH of adsorption and the point of zero charge alone. Undertaking the thermodynamic studies of TCC, the more efficient adsorbent therefore became an interesting endeavor.

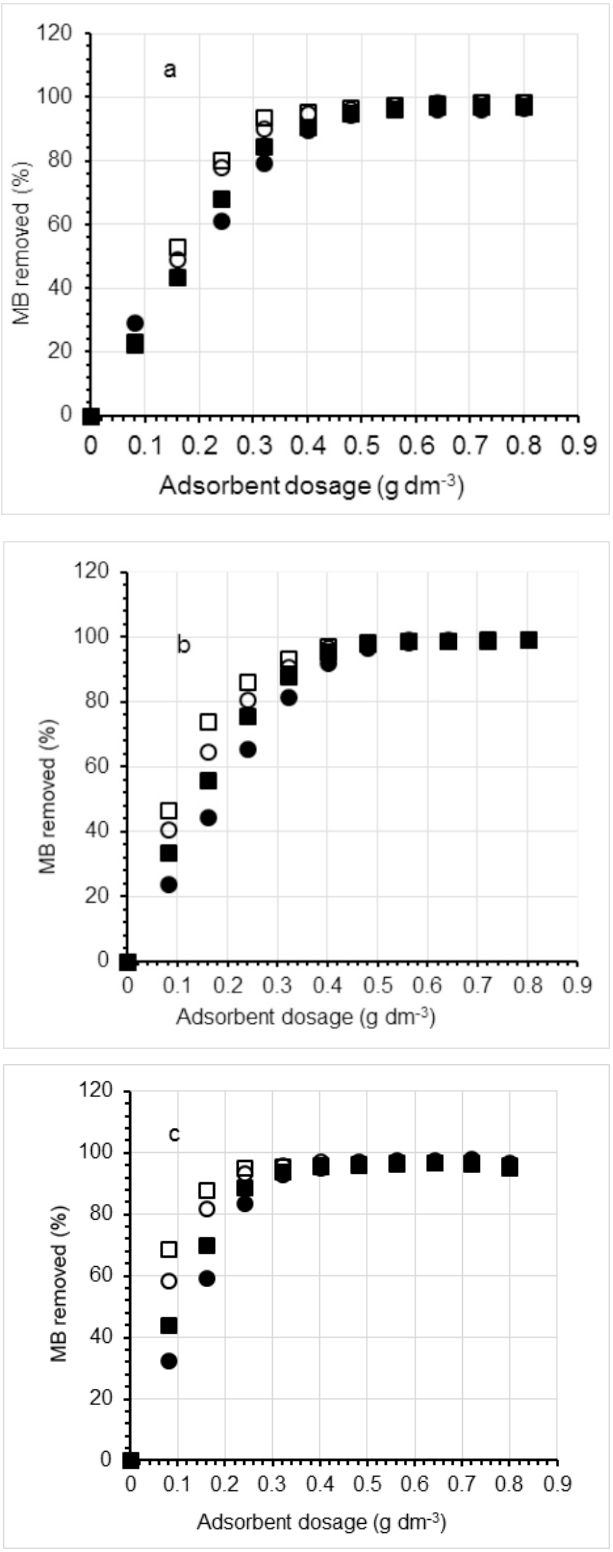

Figure 4: Percentage dye removed as a function of the TCC dosage at 10 °C, filled circle; 20 °C, filled square; 30 °C, open circle; 40 °C, open square. The pH conditions in panel (a) 8.0, (b) 10.5 and (c) 12.0. Initial dye concentration in each case was 47.5 x 10^{-6} mol dm^{-3}. The ionic strength was 0.1 mol. dm^{-3} (NaCl). Each experimental data point is the mean of at least three replicate experiments.

Freundlich, Temkin and Langmuir Adsorption isotherms of MB on TCC

Typical plot of Freundlich isotherm for 25 °C equilibrium experiment at pH 8.0, 10.5 and 12 are presented in Fig. 5a. Corresponding plots for data obtained at other temperature conditions were omitted, but the fitting parameters and the square of the correlation coefficient are presented in Table 1. Corresponding data for Tempkin and the Langmuir isotherms obtained under identical conditions are presented in Figs. 5b and 5c respectively. The fitting parameters of experimental data to those two models are presented also in Table 1 along with the correlation coefficients. Visual inspection of the linear plots (Fig. 5) and the values of the square of the correlation coefficient (R^2) (Tables 1 - 3) reveal that all the plots are sufficiently linear. R^2 was greater than 0.91 in each case, this suggests good reproducibility of all data. Table 1 presents the fitting parameters of Freundlich (according to Eq. 1), Temkin (according to Eq. 2) and Langmuir (according to Eq. 3) model isotherms obtained between 10 and 40 °C at pH 8.0. The fitting parameters were obtained from the linear plot of the appropriate form of the adsorption capacity of TCC and equilibrium concentration of MB in solution. The square of the correlation coefficients are also presented. Corresponding data obtained at pH 10.5 and 12 are presented in Tables 2 and 3 respectively.

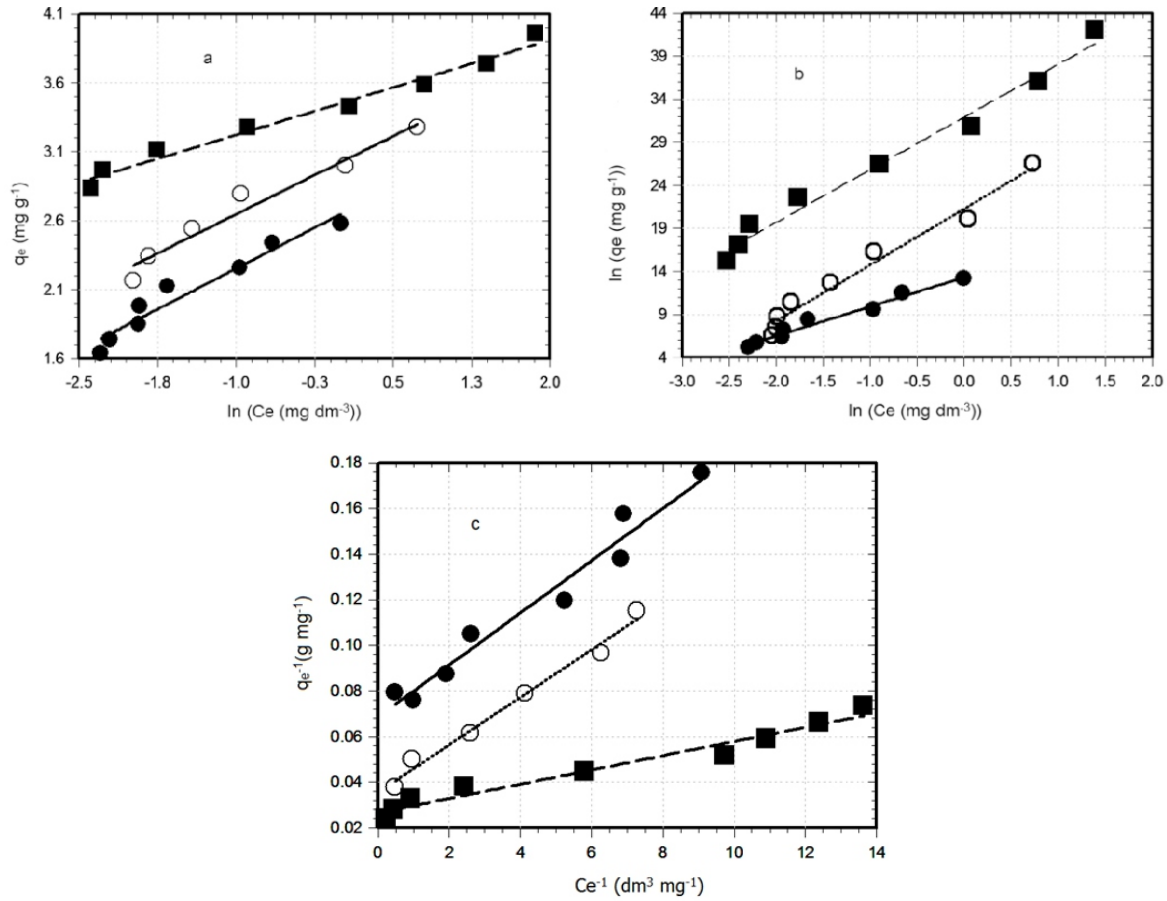

Fig. 5: Dependence of adsorption capacity of TCC on equilibrium concentration of MB as described by linear form of (a) Freundlich (b) Temkin and (c) Langmuir isotherms at 25 °C. Filled circle and full line represent data collected at pH 8.0, squares and broken line represent data collected at pH 10.5 and open circle and dotted line present data collected at pH 12. Other conditions are as described in Fig. 4.

Table 1: Fitting parameters of the equilibrium adsorption of MB on TCC at pH 8.0 to Freundlich Eq. (1), Temkin Eq. (3) and Langmuir Eq. (2)

Model	Freundlich			Temkin			Langmuir		
Temp. °C	K_F ($dm^{3/n}$ $mg^{1-1/n}$ g^{-1})	n^{-1}	R^2	K_T (dm^3 g^{-1})	B_T (J mol^{-1})	R^2	K_L(dm^3 mg^{-1})	q_m (mg g^{-1})	R^2
10	11.018	0.157	0.931	1157.4	1483.1	0.956	8.168	13.018	0.938
15	11.612	0.238	0.964	55.929	779.44	0.958	6.115	13.449	0.969
20	11.960	0.296	0.911	104.25	968.97	0.956	9.033	12.300	0.988
25	14.122	0.394	0.940	49.635	725.69	0.975	5.530	14.976	0.969
30	15.770	0.328	0.958	99.505	780.11	0.985	11.575	14.109	0.978
35	18.527	0.508	0.959	33.462	528.46	0.989	4.556	18.778	0.974
40	26.515	0.565	0.975	44.164	523.28	0.984	6.734	18.050	0.978

Table 2: Fitting parameters of the equilibrium adsorption of MB on TCC at pH 10.5 according to Freundlich Eq. (1), Temkin Eq. (3) and Langmuir Eq. (2)

Model	Freundlich			Temkin			Langmuir		
Temp. °C	K_F ($dm^{3/n}$ $mg^{1-1/n}$ g^{-1})	n^{-1}	R^2	K_T (dm^3 g^{-1})	B_T (J mol^{-1})	R^2	K_L (dm^3mg^{-1})	q_m / mg g^{-1}	R^2
10	23.538	0.133	0.974	10.178	621.89	0.974	8.751	28.571	0.989
15	27.336	0.195	0.961	9.534	462.25	0.958	9.094	34.364	0.945
20	28.801	0.205	0.974	9.045	407.41	0.966	8.029	36.630	0.956
25	31.576	0.229	0.978	8.440	405.14	0.982	7.545	40.161	0.964
30	33.295	0.247	0.977	8.384	354.81	0.973	6.361	43.668	0.955
35	36.227	0.251	0.985	9.386	375.94	0.976	17.875	34.965	0.983
40	37.619	0.311	0.977	7.995	248.29	0.975	5.943	48.077	0.979

Table 3 Fitting parameters of the equilibrium adsorption of MB on TCC at pH 12 according to Freundlich Eq. (1), Temkin Eq. (3) and Langmuir Eq. (2)

Model	Freundlich			Temkin			Langmuir		
Temp. °C	K_F ($dm^{3/n}$ $mg^{1-1/n}$ g^{-1})	n^{-1}	R^2	K_T (dm^3 g^{-1})	B_T (J mol^{-1})	R^2	K_L (dm^3mg^{-1})	q_m (mg g^{-1})	R^2
10	13.042	0.274	0.936	42.737	527.725	0.973	5.221	18.416	0.982
15	15.016	0.426	0.986	28.654	490.210	0.984	2.639	23.981	0.982
20	17.727	0.441	0.946	26.103	447.424	0.9662	2.447	28.985	0.970
25	20.596	0.413	0.933	32.845	380.007	0.974	3.413	28.169	0.985
30	24.653	0.458	0.948	37.565	396.447	0.970	2.311	40.816	0.949
35	26.078	0.520	0.917	24.125	322.471	0.982	2.524	37.736	0.964
40	32.073	0.704	0.942	18.251	241.877	0.995	4.467	6.622	0.999

The following observations are noteworthy about the Freundlich isotherm at all temperature conditions of the experiment: (i) the reciprocal of n which is a measure of adsorption intensity is between 0.133 and 0.71 under the conditions of the experiment (Tables 1 – 3, column 3). This suggests favourable adsorption of MB on TCC under all conditions of the experiment (ii) Freudlinch equilibrium constant, K_F, increases with increasing temperature (column 2, Tables 1 – 3) this is an indication that the affinity of the MB for TCC increases with increasing temperature. Similar result had been reported for the adsorption of Cr(VI) on iron- (III) complex of a carboxylated polyacrylamide-grafted sawdust (Unnithan and Anirudhan, 2001). (iii) At all pHs, the values of reciprocal of n increases with increasing temperature Tables 1 -3, column 3. This gives an indication that the adsorption intensity increases with increasing temperature suggesting that more rooms are made to accommodate the adsorbates with increasing temperature.

Effect of Temperature on the adsorption constants of the three models

Comparing the R^2 for the different models, reveals that the least square regression line through Temkin model is best (in all cases, R^2 is greater than 0.95 (column 7 of Tables 1 – 3)). This is followed by linear fit through Langmuir model as evidenced in columns 4, 7 and 10 (Tables 1 – 3). However, neither of the fitting parameters of Temkin (in column 5) nor of Langmuir (in column 8) shows any significant correlation in relation to temperature (column 1). To confirm this, assuming that values of K_F, K_T and K_L obtained at different temperatures for Freundlich, Temkin and Langmuir isotherm models respectively are identical to equilibrium constant of a chemical reaction, the justification for this assumption is that both equilibrium constant and the constants K_F, K_T and K_L are directly related to the affinity of the adsorbents for the adsorbates. Plots of natural logarithm of the equilibrium values K_X (X is F, T or L) obtained were therefore made as a function of reciprocal of the temperature, according to van't Hoff equation (Fig. 6a – c). In Fig. 6a, Freundlich constant, K_F was used, Figs 6b and 6c make use of Tempkin constant, K_T and Langmuir constant, K_L respectively. The data obtained at different pHs were plotted on the same graph for comparison.

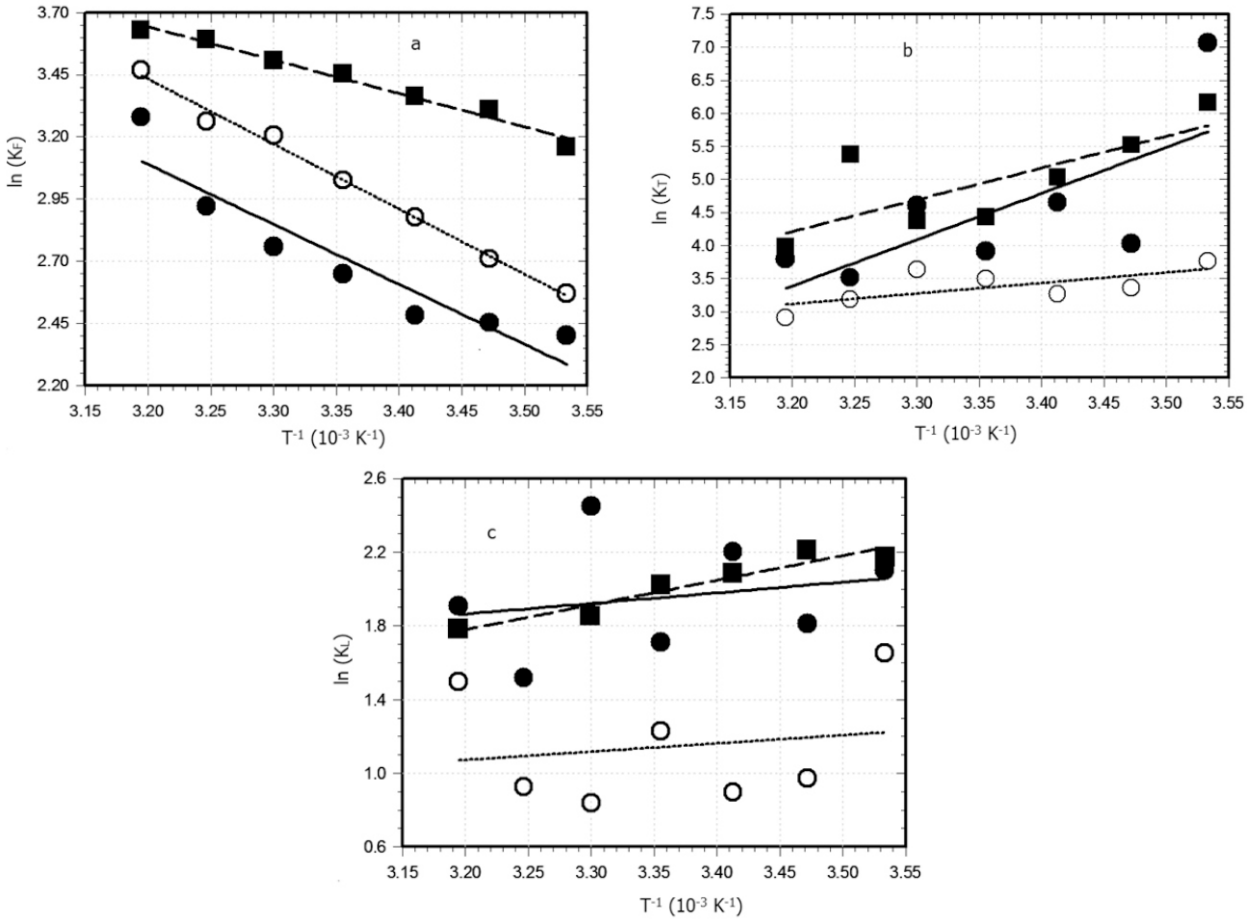

Figure 6. Plot of the natural logarithm of Freundlich constant, K_F, (a) Temkin constant, K_T (b) and Langmuir constant, K_L (c) against the reciprocal of temperature according to Eq. (4). Symbol: Filled circle - pH 8.0; filled square – pH 10.5; open circle - pH 12.

It can be seen that whereas van't Hoff plots using Freundlich constant, K_F (Fig. 6a) are linear at all pH within experimental errors. The correlation coefficient values are 0.939 at pH 8.0, 0.980 at pH 10.5 and 0.993 at pH 12, by contrast, no significant correlation can be seen in the van't Hoff plots using the Temkin constant, K_T (Fig. 6b) or Langmuir constant, K_L (Fig. 6c). In both cases the R^2 are less than 0.6 (Table 4), the only exception was the data fitted using K_L at pH 10.5 for which R^2 was *ca.* 0.91. This suggests that though the R^2 of both Temkin isotherm model (column 7 of Tables 1 - 3) and Langmuir isotherm model (column 10 of Tables 1-3) were better than that of Freundlich (column 4 of Tables 1 - 3), their fitting parameters unlike that of Freundlich model, are not useful in accounting for the thermodynamic properties of the interaction between the adsorbate and the adsorbent.

Enthalpy and Entropy of Adsorption of MB on TCC

The enthalpy and the entropy values evaluated at pH 8, 10.5 and 12 from van't Hoff plots (Fig. 6a) using the Freundlich adsorption constant are presented in Table 4. The value of the standard enthalpy in each case is less than 22 kJ mol^{-1}. Typically, while enthalpy of physical adsorption are less than 25 kJ mol^{-1}, the enthalpy of adsorption of chemisorption are usually > 200 kJ mol^{-1}, which is in the range of bond energy of single covalent bond (Atkins and de Paula 2006; McQuarrie, and Simon, 1997; Silbey *et al.,* 2005). This suggests that the adsoption of MG on to TCC is a physical process (physisorption). This conclusion makes sense, as it point in the same direction with the that from the value of reciprocal of n which was found to be < 1 under all conditions of the experiments. In other to determine the feasibility of the process as a function of the temperature so that comparison can be made with the experimentally observed

adsorption capacities at different pHs, the free energies at different temperatures were calculated using Eq. (5), for the experiments carried out at each pH, and presented in Table 5. It can be seen that in each case, that the free energy change is less than zero and that the magnitude of the free energy change increases with increasing temperature. The increase in adsorption with increasing temperature is particularly more noticeable at low adsorbent dosage (Fig. 4a-c). This finding is qualitatively similar to that reported for adsorption of Cr^{3+}, Cd^{2+} and Pb^{2+} on zea maize seed chaff (Babalola *et al.*, 2016). As the pH changes, it can also be seen from Table 4 also, that the magnitude of the negative value of the free energy change increases in the order ΔG^{o} at pH 8.0 < ΔG^{o} at pH 12.0 < ΔG^{o} at pH 10.5 at any particular temperature, suggesting that the feasibility of the adsorption process is greatest at pH 10.5 and least at pH 8.0. In other words, if the free energy of adsorption at the three pHs of the experiment (pH 8.0, 10.5 and 12.0) are compared, at each temperature, the free energy is least at pH 10.5, indicating that the adsorption process is thermodynamically most feasible at pH 10.5. This observation is in accord with the experimental observation which shows that 99.2% of MB was adsorbed at pH 10.5 while 98.4% and 96.9% are adsorbed at pH 8.0 and 12.0 respectively Fig. 4.

Table 4 Best fit parameters of the line (using K_F) through data points of Fig. 6a with Eq. (4)

pH	($\Delta H^{o}\pm$ SD) / J mol^{-1}	($\Delta S^{o}\pm$ SD) / J K^{-1}mol^{-1}	R^2
8	20040.64±3270.14	89.82±10.99	0.939
10.5	11164.41±707.39	66.01±2.38	0.980
12	21750.02±817.31	98.14±2.75	0.993

SD is the standard deviation.

Table 5 Best fit parameters of the line through data points of Figs. 6 (b and c) with Eq. (4)

	Temkin			Langmuir		
pH	($\Delta H^{o}\pm$ SD)[a] / J mol^{-1}	($\Delta S^{o}\pm$ SD)[a] / J K^{-1}mol^{-1}	R^2	($\Delta H^{o}\pm$ SD)[b] / J mol^{-1}	($\Delta S^{o}\pm$ SD)[b] / J K^{-1}mol^{-1}	R^2
8.0	-58156.71±25687.50	-157.93±86.35	0.506	-4775.23±9411.27	0.22±31.63	0.049
10.5	-39917.66±15096.10	-92.71±50.74	0.5831	-11148.79±1729.36	-20.88±5.85	0.912
12.0	-13209.86±6435.32	-16.37±21.63	0.457	-3728.26±9691.26	-3.02±32.58	0.029

[a]calculated from Temkin model; [b]calculated from Langmuir model.

Table 6 Calculated change in standard free energy change at different temperatures, using the fitting parameters of Table 4, under different pH condition according to Eq. (5).

Temperature	10 °C	15 °C	20 °C	25 °C	30 °C	35 °C	40 °C
ΔG^{o}(pH 8.0) J mol^{-1}	-5378.42	-5827.52	-6276.62	-6725.72	-7174.82	-7623.92	-8073.02
ΔG^{o}(pH 10.5) J mol^{-1}	-7516.42	-7846.47	-8176.52	-8506.57	-8836.62	-9166.67	-9496.72
ΔG^{o}(pH 12) J mol^{-1}	-6023.61	-6514.30	-7005.00	-7495.70	-7986.40	-8477.10	-8967.82

Effect of Acid Treatment on the Adsorbents

It is to be recalled that the difference between TCC and UCC is that in making TCC corncob charcoal was treated with 2 mol dm^{-3} acid whereas no acid treatment was involved in making UCC (Fodeke and Olayera, 2019). Comparing Figs. 3 (presenting adsorption on UCC) and Fig. 4 (presenting adsorption by TCC), one can see that at UCC adsorbent dosage of about 0.8 g/dm^3 (the maximum adsorbent dosage used) the percentage MB adsorbed is *ca.* 81% at pH 9.0 (Fig. 3c) whereas, only 0.3 g/dm^3 of TCC was needed to remove *ca.* 85% of the dye at a pH of 8.0. At lower pH of UCC adsorption medium, the adsorption

efficiency of TCC was almost double that of UCC at identical dosage. The great improvement in the efficiency TCC compared to UCC might have arisen from the removal of bound metal ions and molecules that occupy the binding site of the dye due to acid treatment of the UCC. In the UCC, it is likely that there are fewer site available for adsorption of the dye molecule compared to TCC. It is also possible that the presence of ions on the surface of the UCC adsorbent makes the adsorbent less hydrophobic for MG adsorption. This findings is similar to an earlier report on the adsorption of malachite green to TCC, a major difference however, is that while adsorption of malachite green is an exothermic process, the result here reported is an endothermic process.

Another interesting findings of this work is the discovery that the molar extinction coefficient of MB is pH dependent. The use of the estimated molar extinction coefficient obtained at each pH for the experiment should remove wrong conclusion that may arise from the use of wrong molar absorptivity the study. A number of previous work at different pHs have been carried out using the molar absorptivity of MB in water were used (Ozdemir *et al.* 2009).

At pH 7.2, which is closest pH condition to its point of zero charge (7.55), UCC has adsorption capacity of *ca.* 81% whereas at pH 5.0 (which is 2.55 unit lower than the point of zero charge of the adsorbent), it is only about 58%. At pH 9.0, a pH value which is 1.45 unit higher than the point of zero charge, the maximum adsorption capacity is *ca.* 81%. This high adsorption capacity might not be unconnected to the combination closeness of the surface charge at this pH to the PZC as evidenced in Fig. 1 and the adsorption favourable electrostatic repulsion between the ions of solution and MB at alkaline pH. At pH 5.0 however, repulsion between adsorbed positively MB and the one in solution has tendency to reduce the adsorbent affinity for more MB. The difference in the adsorption capacities of each adsorbent under different pH conditions suggests that the adsorption capacities of each adsorbent increase with the closeness of the pH condition to the point of zero charge. This may be rationalized on the ground that both the point of zero charge of the adsorbent and the net charge on the adsorbate surface charge play important role in the adsorption process. The adsorption capacity of the adsorbent for MB molecules should increase when the repulsive interaction between dye molecules solution increase and when repulsion between adsorbate and adsorbent is minimum. It goes to say that at the ionic strength of 0.1 mol. dm^{-3} (NaCl) of the solution, the separation between the micropores on the surface of the adsorbent is greater than the ionic atmosphere of the bound MB. Therefore, the charge on neighbouring MB species bound to the adsorbent might have been significantly screened off. Therefore, at pH below the point of zero charge, the adsorption capacities should be weak, but increase to maximum around the point of zero charge after which it should reduce more significantly due to electrostatic repulsion between neighbouring dye molecules. Another justification for this findings, is that in addition to the counter ion on MB being screened off, the molecules which is largely hydrophobic gets more attracted to the adsorbent surface whose hydrophobicity increases and peaks around the point of zero charge. This might account for why the adsorption capacity of the adsorbent for the adsorbate increases as the point of zero charge is approached and decreases above it. (Figs. 4B and 4C)

Another intriguing finding from the thermodynamic studies of the interaction of MB with TCC is that determination of the optimum isotherm fit for an adsorption system by merely comparing the R^2 of series of isotherm models could lead to erroneous conclusion about the most suitable isotherm model. It is now evident that a suitable isotherm model, in addition to having a sufficiently high R^2 (usually greater than 0.9), should be able to within experimental uncertainty, account for the thermodynamic properties of the adsorption process of the system. In other words, in addition to having a high correlation coefficient, the thermodynamic quantities obtained by fitting the equilibrium fitting parameter, analogous to equilibrium constant, must be able to account for the observed adsorption properties. This findings is consistent with the report that size of error function alone is inadequate for deciding the optimum isotherm of an adsorption process (Kumar *et al.*, 2008). In

addition to the size of error function, the theory behind the isotherm should be verified with experimental data (Kumar *et al.*, 2008). In the report here presented we confirmed that both the thermodynamic quantities obtained and the observed adsorption properties of the system are consistent with the Freudlich isotherm though its R^2 from its isotherms were slightly lower than those of Temkin and Langmuir, which neither gave a reasonable van't Hoff fit for the estimation of the thermodynamic quantities nor were unable to account for the observed adsorption behavior of the system.

CONCLUSION

It was demonstrated that acid treatment of corncob charcoal significantly enhances it adsorption capacity for MB. It was also shown that the molar absorptivity of MB was pH dependent and that using the molar absorptivity of MB dye in water for experiments at acidic or alkaline pH could lead to erroneous result. The most important finding is that higher correlation coefficient value from an isotherm model fit to an equilibrium data of adsorbent-adsorbate sorption experiment alone should not be used as a conclusive test of the most suitable model fit for an adsorption system. Thermodynamic studies should be carried to ensure that such model could account for the observed sorption properties.

ACKNOWLEDGEMENT

We are grateful to Mr. S. S Durodola and Mr. Shina Ramoni of the Department of Chemistry, Obafemi Awolowo University for technical support provided.

REFERENCES

Adegoke, K.A. and Bello O.S. 2015. Dye sequestration using agricultural wastes as adsorbents *Water Resources and Industry,* 12, 8–24.

Amodu, O.S., Ojumu, T.V., Ntwampe, S.K. and Ayanda, O.S. 2015. Rapid Adsorption of Crystal Violet onto Magnetic Zeolite Synthesized from Fly Ash and Magnetite Nanoparticles. *Journal of Encapsulation and Adsorption Science,* 5, 191-203.

Atkins, P and de Paula J. 2006. Physical Chemistry, 8th Ed. Oxford University Press, New York, pp 917

Ayad, M.M., El-Nasr, A.A and Stejskal, J. 2012. Kinetics and isotherm studies of methylene blue adsorption onto polyaniline nanotubes base/silica composite. *Journal of Industrial and Engineering Chemistry,* 18, 1964-1969.

Babalola, J.O., Omorogie, M.O., Babarinde, A.A., Unuabonah, E.I. and Oninla, V.O. 2016. Optimization of the biosorption of Cr^{3+}, Cd^{2+} and Pb^{2+} using a new biowaste: Zea mays seed chaff. *Environmental Engineering Management Journal*, 12(7), 1571 - 1580

Bakatula, E.N., Richard,D., Neculita., C.M. and Zagury, G.J., 2018. Determination of point of zero charge of natural organic materials Environmental Science and Pollution Research https://doi.org/10.1007/s11356-017-1115-7

Bello, O.S., Adeogun, I.A., Ajaelu, J.C. and Fehintola, E.O. 2008. Adsorption of methylene blue onto activated carbon derived from periwinkle shells: kinetics and equilibrium studies. *Chemistry and Ecology*, 24, 285 – 295

Chen, Z., Zhang. J. and Wang, J.F.M., Wang, X., Han, R. and Xu, Q. (2014). Adsorption of methylene blue onto poly(cyclotriphosphazene-co-4,4 - sulfonyldiphenol) nanotubes: kinetics, isotherm and thermodynamics analysis, *Journal of Hazardous Materials,* 273, 263-271

Fernandez-Pe´rez, A. and Marba´n, G. 2020. Visible Light Spectroscopic Analysis of Methylene Blue in Water; What Comes after Dimer? *ACS Omega*, 5, 29801–29815,

Fodeke, A.A. and Olayera, O.O. 2019. Thermodynamics of Adsorption of malachite green hydrochloride on treated and untreated corncob charcoal. *Journal of Serbian Chemical Society*, 84, 1143 – 1154.

Freundlich, H.M.F. 1906. Over the adsorption in solution, *Zeitschriftf¨urPhysikalischeChemie*, 57A, 385.

Garg, V.K., Amita, M., Kumar, R and Gupta, R. 2004. Basic dye (methylene blue) removal from simulated wastewater by adsorption using Indian Rosewood sawdust: a timber industry waste. *Dyes and Pigments*, 63, 243-250

Golz, E.K., and Vander Griend, D.A. 2013. Modeling Methylene Blue Aggregation in Acidic Solution to the Limits of Factor Analysis. *Analytical Chemistry*, 85(2), 1240–1246. doi:10.1021/ac303271m

Kano, F., Abe, I., Kamaya, H., and Ueda, I. 2000. Fractal model for adsorption on activated carbon surfaces: Langmuir and Freundlich adsorption. *Surface Science*, 467, 131–138

Kumar, K.V, Porkodi, K., and Rocha. F., 2008. Isotherms and thermodynamics by linear and non-linear regression analysis for the sorption of methylene blue onto activated carbon: Comparison of various error functions. *Journal of Hazardous Materials,* 151, 794-804

Langmuir, I. 1916. The constitution and fundamental properties of solids and liquids, *Journal of American Chemical Society*, 38, 2221.

McQuarrie, D.A and Simon, J.D. 1997. Physical Chemistry: A Molecular Approach, University Science Books, USA. pp 1295 – 1296

Malik, R., Ramteke, D.S. and Wate, S.R. 2007. Adsorption of malachite green on groundnut shell waste based powdered activated carbon, *Waste Management,* 27, 1129–113

Ozdemir, F. A., Demirata, B., and Apak, R. 2009. Adsorptive removal of methylene blue from simulated dyeing wastewater with melamine-formaldehyde-urea resin. *Journal of Applied Polymer Science,* 112(6), 3442–3448. doi:10.1002/app.29835

Rajesh, W., Sivakumar, S., Senthilkumar, P. and Subburam, V. 2001. Carbon from cassava peel, an agricultural waste, as an adsorbent in the removal of dyes and metal ions from aqueous solution, *Bioresouresource Technology*, 80, 233–235.

Silbey, R.J. Alberty, R.A. and Bawendi, M.G. 2005. Physical Chemistry, 4th Ed. John Wiley and Sons, Inc. USA. pp 840 – 841.

Suteu, D., Malutan, T. and Bilba, D. 2011. Agricultural waste corn cob as a sorbent for removing reactive dye orange 16: equilibrium and kinetic study. *Cellulose chemistry and technol*ogy 45**,** 413-420

Tan, W. F., Lu, S. J., Liu, F., Feng, X. H. and He, J. Z. 2008. Determination of the point of zero charge of manganese oxides with different methods including an improved salt titration method. *Journal of Soil Science*, 173, 277–286.

Temkin, M.I. and Khim, Z.F. 1914. Adsorption equilibrium and the kinetics of processes on nonhomogeneous surfaces and in the interaction between adsorbed molecules. *Russian Journal of Physical Chemistry*, 15, 296.

Unnithan, M.R., and Anirudhan, T.S. 2001. The Kinetics and Thermodynamics of Sorption of Chromium (VI) onto the Iron (III) Complex of a Carboxylated Polyacrylamide-Grafted Sawdust. *Industrial and Engineering Chemistry Research,* 40(12), 2693–2701.